

Coupling atomistic and continuum hydrodynamics through a mesoscopic model: Application to liquid water

Rafael Delgado-Buscalioni,^{1,a)} Kurt Kremer,^{2,b)} and Matej Praprotnik^{2,c)}

¹*Departamento Física Teórica de la Materia Condensada, Universidad Autónoma de Madrid, Campus de Cantoblanco, E-28049 Madrid, Spain*

²*Max-Planck-Institut für Polymerforschung, Ackermannweg 10, D-55128 Mainz, Germany*

(Received 11 May 2009; accepted 17 November 2009; published online 28 December 2009)

We have conducted a triple-scale simulation of liquid water by concurrently coupling atomistic, mesoscopic, and continuum models of the liquid. The presented triple-scale hydrodynamic solver for molecular liquids enables the insertion of large molecules into the atomistic domain through a mesoscopic region. We show that the triple-scale scheme is robust against the details of the mesoscopic model owing to the conservation of linear momentum by the adaptive resolution forces. Our multiscale approach is designed for molecular simulations of open domains with relatively large molecules, either in the grand canonical ensemble or under nonequilibrium conditions. © 2009 American Institute of Physics. [doi:10.1063/1.3272265]

I. INTRODUCTION

Many relevant properties of condensed matter require understanding how the physics at the nanoscale (nanometer and nanosecond) builds up or intertwines with structures and processes on the microscale (micrometer and microsecond) and beyond. The so called *multiscale modeling* techniques have been rapidly evolving during the last decade to bridge this gap. The “multiple-scale” problem is common to many different disciplines, and a variety of multiscale models is being designed to tackle different scenarios either in solids^{1,2} or soft matter.^{3–6} The main objective of multiscale modeling of complex fluids is to study the effect of large and slow flow scales on the structure and dynamics of complex molecules (e.g., polymers, proteins), or complex interactions (e.g., liquid-solid interfaces, wetting fronts, structure formation, etc.). In this context, multiscale modeling is usually based on *domain decomposition*: a small part of the system [$O(10$ nm)] is solved using fully fledged (classical mechanics) atomistic detail and it is coupled to a (much larger) outer domain, described by a coarse-grained (either particle or continuum) model. The central idea of these “dual-scale” methods is to solve large and slow processes using a computationally low demanding description, while retaining an atomistic detail only where necessary.

As a natural step, some recent works have started to explore how to include a “mesoscopic layer” to act as an interface between the atomistic and continuum regions. These “triple-scale” models have been presented for algorithms based on flux exchange⁷ and state-exchange coupling.⁸ Indeed the choice of a particular method depends on the problem under consideration. Flux-exchange algorithms respect conservation laws by construction and thus

can be designed to exactly conserve mass, momentum, and energy.^{9,10} This, however, requires concurrent temporal coupling, i.e., to keep the same clock in all the domains. State exchange is based on the Schwartz method, which alternatively imposes the local velocity of the adjacent domain at the overlapping layer until the steady state is reached. Also, the number of particles in each domain is held constant (i.e., the fluid is assumed to be incompressible) and mass flow across the particle region is controlled by the convective transport in its continuum (averaged) form.^{8,11} Thus, apart from a different temporal coupling, the state-exchange strategy is based on a “top-down” approach, which successfully introduces the mean flow state into the microscopic boundary.

In this work we follow a different route which intends to retain as much as possible molecular information into the triple-scale coupling. To that end, we adopt a flux-exchange strategy. From the molecular side of the problem, an important application of domain decomposition is the study of open systems, having a nonconstant number of molecules. A dynamic coupling requires to “open up” a molecular dynamics (MD) domain to exchange mass, momentum, and energy according to the underlying microscopic dynamics which, not only should carry information on the average convective transport, but also on the molecular diffusion across the open boundary. Also, in this “bottom-up” approach the spatial molecular arrangement should be conserved in the mesoscopic domain as well. As a significant test, at equilibrium, mass fluctuations across the MD-mesoscopic boundary should be thermodynamically consistent with the fluid compressibility. A formulation for flux exchange across open boundaries in particle systems is already available⁹ and was shown to allow for MD simulations in different types of thermodynamic ensembles. The triple-scale scheme presented in this work is equipped with this idea, which permits to study the dynamics of confined (yet open) molecular systems evolving toward the grand canonical (GC) equilibrium ensemble (see e.g.,

^{a)}Electronic mail: rafael.delgado@uam.es.

^{b)}Electronic mail: kremer@mpip-mainz.mpg.de.

^{c)}Electronic mail: praprot@cmm.ki.si. On leave from the National Institute of Chemistry, Hajdrihova 19, SI-1001 Ljubljana, Slovenia.

Ref. 12). In passing we note that the existing Monte Carlo¹³ (MC) or hybrid MC-MD algorithms¹⁴ for the GC ensemble can only provide restricted dynamical information of the system.

Coming back to dual-scale models, the first class of domain decomposition to appear was based on particle-continuum coupling (see Ref. 4 for a review). Unsteady flow can be solved by hybrids based on exchanging the momentum flux across the interface (H) between the MD domain and a continuum fluid dynamics (CFD) solver. One of these schemes (HybridMD) implements an open-boundary formulation⁹ and extends the formalism to deal with hydrodynamic fluctuations across H and inside the CFD domain.^{10,15} However, the particle insertion used by original “open MD” scheme was restricted to small solvent molecules, such as argon or water,¹⁶ due to the large steric hindrance of any atomistic complex molecule description.

More recently, another type of domain decomposition based on particle-particle coupling appeared. The Adaptive Resolution Scheme (AdResS)^{3,17} couples a coarse-grained particle model with its corresponding atomistic description. To do so, the number of degrees of freedom (DoFs) of the molecules is adapted (reduced/increased) as molecules move across a “transition” layer where the all-atom explicit model (*ex*) and the coarse-grained (*cg*) model are gradually switched on/off, through a hybrid model (*hyb*). The great benefit of AdResS resides in making feasible the gradual (on-the-fly) transition of a complex molecule description: from a coarse-grained potential with soft intermolecular interactions to an atomistic one, with the whole set of hard cores.

We realized that taking the advantages of HybridMD and AdResS should then have a symbiotic effect, potentially solving most of the limitations of each method. In a recent article⁷ we started to explore in such direction and applied the combined AdResS-HybridMD model to a liquid of simple tetrahedral molecules. By performing molecule insertion within the *cg* domain, the combined scheme enables to simulate an open MD system and couples its dynamics to a continuum flow description of the outer region. However, the coupling strategy used in Ref. 7 does not avoid some drawbacks already present in the original setup of the AdResS scheme.¹⁷ In particular, a precise mapping of structural and dynamical properties of the *cg* and *hyb* molecules^{18–21} was still required. Hence, any simulation exploring a new thermodynamic state requires new calibrations of the coarse-grained models (in practice, each simulation is restricted to sample one single thermodynamic state).

In the present work we show that the coupling geometry can be modified to yield a more flexible and robust AdResS-HybridMD scheme. This new implementation avoids the burden associated with the fine tuning of coarse-grained layers, thus relieving a great deal of the specificity of the coarse-grained model. This is important not only from the computational standpoint, but also because it opens a route to consider processes along a thermodynamic path. A general completion of this route requires the inclusion of the energy exchange into the combined scheme, and some possible solutions are hereby suggested. Section II briefly introduces the

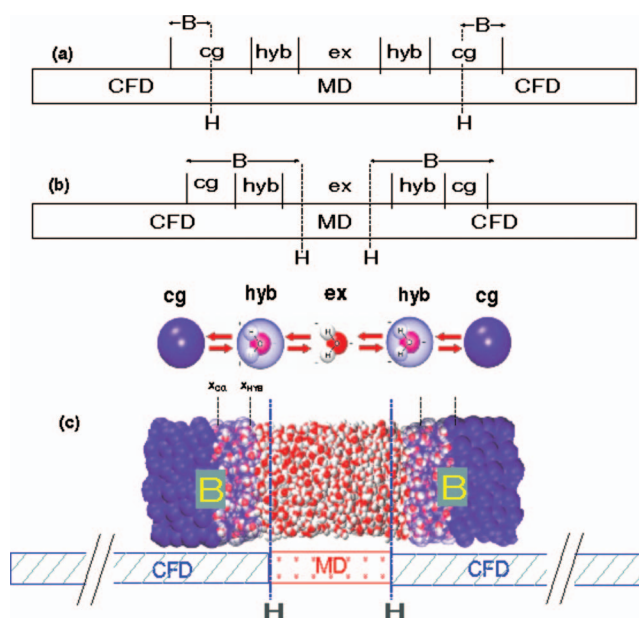


FIG. 1. Coupling strategies for the AdResS-HybridMD scheme: (a) coarse-grained buffer and (b), (c) adaptive resolution buffer. In each figure, the bottom panel depicts the decomposition of the whole system (MD+CFD); where MD stands for the molecular dynamics region surrounded by CFD domains solved via the finite volume method (Ref. 22). The MD-CFD coupling is solved by the HybridMD scheme (Ref. 15) based on the exchange of momentum flux across the interface H. Pressure and stress are imposed into MD via external forces acting on particles at the buffers B. The AdResS scheme (Ref. 3) (see the middle figure) gradually adapts the atomic resolution of the molecules: from all-atom (*ex*) to coarse-grained (*cg*) descriptions, passing through a hybrid (*hyb*) model. AdResS and HybridMD can be combined in two ways depending on location of the interface H: either using a coarse-grained buffer (a), see Ref. 7, or an adaptive resolution buffer (b) and (c), explored in this work. (c) is an illustration of this triple-scale scheme for liquid water. The hydrodynamic coupling is made along x direction, (finite volume cells are $\Delta x = 3.5\sigma$ wide) and the system is periodic in the orthogonal directions. The atomic resolution of water molecules is gradually switched on as they move across the buffer, which is 7σ long. The *hyb* region is 3.5σ and its distance to H is about 1σ . A standard DPD thermostat at $T=300$ K is used for the *cg* and *hyb* domains, with a friction constant $\zeta=0.5$ m/ τ . Information between MD and CFD is exchanged after every fixed time interval Δt_c , with $\Delta t_c = n_{\text{CFD}} \Delta t_{\text{CFD}} = n_{\text{MD}} \delta t$. Here we typically used $\Delta t_c = \Delta t = 0.03\tau$ and $\delta t = 0.00037\tau = 0.5$ fs (small enough to recover O–H vibrational motion).

(dual scale) hybrid models (HybridMD and AdResS). Coupling strategies are explained in Sec. III and simulations and results are presented in Secs. IV and V. Some conclusions are given in Sec. VI.

II. HYBRID MODELS

A. Particle-continuum hybrid (HybridMD)

The HybridMD^{10,15} scheme couples the hydrodynamic of a particle region, here called MD domain, with a CFD of the external fluid. The essential quantity exchanged between CFD and MD is the momentum flux across the MD-CFD interface H (see Fig. 1), which can be casted as $\mathbf{J}_H \cdot \mathbf{n}$, where \mathbf{J}_H is the local pressure tensor and \mathbf{n} is the unit vector normal to the H interface, whose area is A . The momentum flux is transferred to the MD domain by imposing an external force $\mathbf{F}^{\text{ext}} = A \mathbf{J}_H \cdot \mathbf{n}$ to a particle buffer (the overlapping domain B in Fig. 1) adjacent to the MD domain. Molecules are free to cross the H interface, from or toward the buffer, but once in

B, each molecule i feels an external “hydrodynamic” force distributed according to $\mathbf{F}_i^{\text{ext}} = g(x_i)\mathbf{F}^{\text{ext}}/\sum_{i \in B} g(x_i)$, where x is the coordinate normal to H. Several options can be chosen for the distribution function,¹¹ we used a step function $g(x) = \Theta(x - x_o)$, as in Ref. 10.

Through the interface H, the CFD domain receives exactly the same amount of momentum as the MD system does, but in opposite direction, thus ensuring conservation. Also, the particle’s mass crossing H is injected into the CFD domain via a relaxation procedure.¹⁵ This means that conservation of total mass and momentum only applies to the system MD+CFD. In other words, strictly speaking B is not part of the total system¹⁰ and can be thought of as a particle reservoir where we apply flux boundary conditions to the MD system. Finally, we note that the only “microscopic” information required at the CFD level is the equation of state and viscosities of the atomistic fluid (Here, we assume that the constitutive relation is known.).

B. Adaptive resolution scheme (AdResS)

As stated, the AdResS scheme couples an atomistic domain and a coarse-grained particle region by adapting, on-the-fly, the molecular description of those molecules moving across both domains. This is clearly illustrated in Figs. 1(b) and 1(c), where the atomistic domain is labeled as *ex*, the coarse-grained region as *cg*, and *hyb* denotes the transition region between both domains. In this transition regime, the force acting on a molecule is a hybrid of the explicit and coarse-grained forces,

$$\mathbf{F}_{\alpha\beta} = w(X_\alpha)w(X_\beta)\mathbf{F}_{\alpha\beta}^{\text{atom}} + [1 - w(X_\alpha)w(X_\beta)]\mathbf{F}_{\alpha\beta}^{\text{cm}}, \quad (1)$$

where $\mathbf{F}_{\alpha\beta}$ is the intermolecular force acting between centers of mass of molecules α and β , placed at $x = X_\alpha$ and X_β in the coupling coordinate, $\mathbf{F}_{\alpha\beta}^{\text{atom}}$ is the sum of all pair intermolecular atom interactions between explicit atoms of the molecules α and β , $\mathbf{F}_{\alpha\beta}^{\text{cm}} = -\nabla_{\alpha\beta} U^{\text{cm}}$ is the corresponding coarse-grained force acting on the center of mass of the molecule (cm), and w is the weighting function determining the degree of resolution of the molecules. The value $w=1$ corresponds to the *ex* region, $w=0$ to the *cg* region, while values $0 < w < 1$ corresponds to hybrid (*hyb*) models. In this study we used the same functional form of w as in Ref. 7.

Each time a molecule leaves (or enters) the coarse-grained region it gradually gains (or loses) its equilibrated vibrational and rotational DoFs while retaining its linear momentum. Note that the change in resolution carried out by AdResS is not time reversible as a given *cg* molecule corresponds to many orientations and configurations of the corresponding *ex* molecule. Since time reversibility is essential for energy conservation,²³ AdResS does not conserve energy. In particular, the force in Eq. (1) is in general not conservative in the *hyb* region (i.e., in general $\oint \mathbf{F}_{\alpha\beta} \cdot d\mathbf{r} \neq 0$).^{24,25} Hence, to supply or remove the latent heat associated with the switch of resolution we employ a standard dissipative particle dynamics (DPD) thermostat^{26,27} acting at the *cg* and *hyb* regions. Note that the thermostat forces do not enter into the AdResS interpolating scheme, Eq. (1). Instead, they are added separately.¹⁷

III. COUPLING STRATEGIES

The AdResS-HybridMD scheme can be applied in several contexts. In general terms, the scheme solves the hydrodynamic coupling of a MD system with external (CFD) flow. This goal requires hydrodynamic consistency (e.g., momentum conservation). Also, a reduced, but yet important, application of the combined scheme consists on the study of the equilibrium MD of open systems with relatively large molecules. For this sake thermodynamic consistency is required; in particular sampling the grand-canonical ensemble requires proper mass fluctuations across the simulation boundaries. Confined systems are a relevant example of this sort of application (see e.g., Ref. 12), for which the role of CFD domain can be simplified to just provide the external pressure (and temperature) of the external mass reservoir.

In the same way, the geometry used for the AdResS-HybridMD coupling allows for a certain flexibility; the key issue being the location of the interface H connecting the MD and CFD domains (see Fig. 1). In a previous work⁷ we proposed to place the H interface within the coarse-grained domain [see Fig. 1(a)]. This setup is useful to include hydrodynamics in simulations requiring a particle-based multiscale description (e.g., using AdResS). An example of application could be the study of the dynamics of ions nearby a charged surface under flow conditions; here the *ex* layer would describe the physics near and at the surface, while away from it, charged *cg* particles will eventually transfer the external flow from the outer CFD region.

On the other hand, many studies are focused on the atomistic region and do not really require a particle-based multiscale description around it. In these cases, a more logical setup is to place the interface H within the atomistic domain *ex* [see Figs. 1(b) and 1(c)]. In this paper we explore the benefits of this second coupling strategy which, as stated, might open a route to consistently couple the hydrodynamics and thermodynamics of qualitatively different levels of description.

A. Coarse-grained buffer

A detailed description of this setup, which locates the hybrid interface H into the *cg* domain [see Fig. 1(a)], can be found in Ref. 7; we now briefly summarize its requirements. In this setup the original AdResS scheme is implemented *inside* the MD domain. Thus, the first requirements of this coupling geometry are demanded by AdResS.¹⁷ In particular, to guarantee a similar fluid structure along the AdResS layers, one needs to calibrate the radial distribution function (RDF) and equation of state of the coarse-grained model *cg* and *hyb* so as to fit the atomistic fluid values. The *cg* pressure was fitted by introducing a linear correction term which only affects the long-range part of each pair interaction (see Ref. 18 and Refs. 28 and 29 for application to simple liquids). We note that the RDF is, however, essentially determined by short-range interactions. To ensure a flat pressure profile along the hybrid (*hyb*) domain, extra pressure corrections require also the same type of calibrations for the intermediate hybrid model $w = \frac{1}{2}$. Finally, hydrodynamic consistency demands to take care of the viscosities of the *cg* and

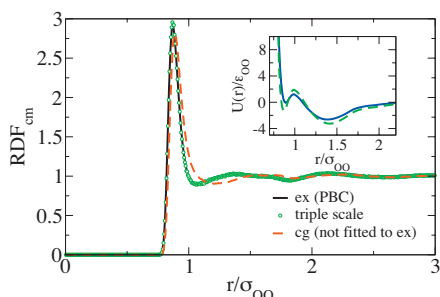


FIG. 2. Comparison between RDF_{cm} s obtained in an all-atom (*ex* model) periodic boundary simulation of the flexible TIP3P water at ambient conditions and within the MD region of a triple-scale simulation. At the buffer we used a *cg* model whose RDF_{cm} (dashed line) was not fitted to the all-atom result. The inset shows the effective potentials $U_{w=0}^{\text{cm}}$ and $U_{w=0.5}^{\text{cm}}$ used in the first protocol (see text), which correctly reproduce the all-atom RDF_{cm} : two minima corresponding to the first and second hydration shells of the liquid are observed.

hyb models,⁷ and fit them to the *ex* fluid value¹⁹ (as shown in Ref. 7 this does not guarantee a perfect fit of the diffusion coefficients). In summary, for each thermodynamic state considered, one needs to perform the following calibration steps.

- (1) Calibrate the effective potential $U_{w=0}^{\text{cm}}$ of the *cg* model¹⁸ so as to fit the center-of-mass RDF (RDF_{cm}) and pressure of the *ex* model³ (solid line in the inset of Fig. 2);
- (2) The interface pressure correction²⁸ is used to suppress density oscillations in the *hyb* layer. This requires the calibration of the effective potential $U_{w=0.5}^{\text{cm}}$ for the hybrid model with $w=\frac{1}{2}$ (dashed line in the inset of Fig. 2); and
- (3) Measure the viscosity of the *cg* model then calibrate the transverse friction coefficient of the transverse DPD thermostat¹⁹ so as to match η_{cg} and η_{ex} . This requires several viscosity calculations.⁷

B. Adaptive resolution buffer

The setup discussed in this work consists on placing the hybrid interface H inside the atomistic domain [see Figs. 1(b) and 1(c)]. In this setup AdResS works *inside the buffer*. The MD region is thus purely atomistic and this fact brings about an important benefit; around the hybrid interface H, all relevant fluid properties are properly defined. These include the fluid transport coefficients, energy and pressure equation of states, and the corresponding mass and pressure fluctuations. In this context, MD-CFD coupling by HybridMD is well defined.¹⁵ On the other side, by placing AdResS into the particle buffer it behaves as an *adaptive resolution buffer*, where the atomistic DoFs are gradually inserted into the MD (atomistic) region of interest. Note that the *cg* layer, with soft interaction potentials, is placed near the buffer end [see Figs. 1(b) and 1(c)], so the insertion of complex molecules into the system is still an easy task, using standard insertion routines.³⁰ The computational costs of the presented setup of the method are the same as in the coarse-grained buffer setup.⁷

The second relevant benefit of this coupling strategy is that it permits to properly impose the external pressure and stress into MD, without having to perform a fine tuning of

the structural and dynamic properties of the *cg* and *hyb* models. In other words, the AdResS-HybridMD scheme does not rely on the specificity of the coarse-grained description anymore. The reason for this is simple: the AdResS scheme conserves linear momentum. This means that any external momentum flux will be properly transferred across the AdResS layers to the atomistic core. As the external “hydrodynamic” force used in the HybridMD scheme decouples from any intermolecular interaction (the total force on a molecule at the buffer B is $\mathbf{F}_\alpha = \mathbf{F}_\alpha^{\text{ext}} + \sum_\beta \mathbf{F}_{\alpha\beta}$), the transfer of mechanical variables (pressure and stress) should be robust against the details of the *cg* and *hyb* models. However, to avoid a large imbalance between the external pressure (provided by external forces) and the *cg* thermodynamic pressure, it is preferable to work with *cg* potentials providing a reasonably good fit of the *ex* pressure, rather than a finely tuned RDF (moreover, the feasibility of matching both the pressure and the RDF of any fluid, from coarse-grained pairwise interactions, is still a subject of discussion^{18,31}). A way to construct this sort of effective potentials for large molecules was presented in Ref. 32. We now present simulations to prove the robustness of the scheme with respect to mechanics (pressure, velocity) and thermodynamic variables (mass fluctuations), and also check any possible effect on the liquid structure near the interface H.

IV. SIMULATIONS

The present hybrid simulations were implemented for the flexible TIP3P water model, partly because of the relevance of water and also because it has well known structural and dynamical properties.^{22,33–35} In the remainder of the paper we use reduced Lennard-Jones units corresponding to the oxygen atom: mass $m=m_{\text{O}}=16$ a.u., oxygen-oxygen interaction energy $\epsilon=\epsilon_{\text{OO}}=0.152\,073$ kcal/mol, and diameter $\sigma=\sigma_{\text{O}}=3.1507$ Å. Simulations were done at ambient temperature, $T=300$ K, which corresponds to $k_{\text{B}}T/\epsilon=3.92$ in reduced units. TIP3P-water density is 1.02 gr/cm³, which corresponds to $\rho=1.20$ m/σ^3 . Most particle simulations were done in boxes of total (MD+B) volume $24.5 \times 6.18 \times 11.12\sigma^3$, although in order to check for finite size effects, boxes with larger dimensions were also used. The volume of the MD domain was $V=10.5 \times 6.18 \times 11.12\sigma^3$ and it contained about 865 water molecules. Long-range electrostatic forces are computed using the reaction field method, in which all molecules outside a spherical cavity of a molecular based cutoff radius $R_c=2.86\sigma$ are treated as a dielectric continuum with a dielectric constant $\epsilon_{\text{RF}}=80$.^{28,36,37} The finite volume solver for the CFD domain was fed with the equation of state for flexible TIP3P water reported in Ref. 22. Finally, the microscopic part of the stress tensor at the hybrid interface H was measured according to the mesoscopic approach explained in Ref. 10, i.e., by evaluating velocity gradients from the cell-averaged particle velocities and using the Newtonian constitutive relation.

V. RESULTS

Coarse-grained buffers. As expected, results proved the correct behavior of the combined scheme, both in terms of

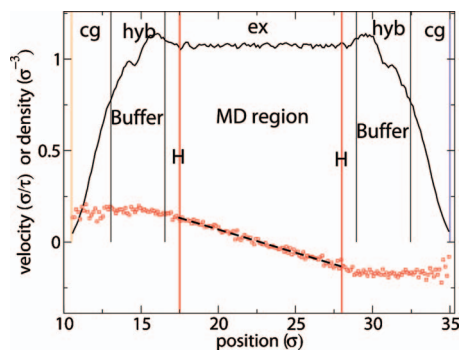


FIG. 3. Density profile (solid line) and velocity distribution (squares) across the particle domain in a steady Couette flow (the dashed line is the expected linear profile across the MD region).

the structure and hydrodynamics at the MD domain. However, calibration steps, using the recipe explained in Sec. III A, involved significant work. Strong corrections of the *cg* and *hyb* viscosities¹⁹ were required (without transverse DPD thermostat, η_{cg} is about five times smaller than η_{ex}). In these calibration steps we used HybridMD as a rheometer.¹⁰

Adaptive resolution buffers. In what follows we focus on the result obtained for the second, much lighter setup. It is important to stress that these simulations were done using an effective potential for the *cg* model, which was deliberately not accurately fitted to reproduce the all-atom RDF_{cm} (see Fig. 2). Moreover, steps 2 and 3 of the protocol of Sec. III A were also avoided, meaning that the shear viscosities at the *cg* and *hyb* layers result in much smaller values than the atomistic (*ex*) one.

A. Liquid structure

We first compare, in Fig. 2, the local structure of the liquid inside the MD region of the triple-scale model with that obtained from all-atom simulations within periodic boundaries. The agreement is perfect, indicating that the unfitted liquid structure in the buffer (dashed line in Fig. 2) does not affect the proper liquid structure inside the interest (MD) region.

B. Hydrodynamics

The hydrodynamic behavior of the triple-scale scheme was tested considering both steady and unsteady flows. Figure 3 shows the density and velocity profiles in the particle region (MD+B) obtained at the steady state of a simple Couette flow. The density (and temperature, not shown) profile inside the MD region is flat and confirm that the triple-scale scheme furnishes a homogeneous equilibrated liquid bulk. The expected linear velocity profile inside the MD domain indicates that the transverse momentum is correctly transferred across the triple-scale fluid model. We also conducted simulations of Stokes flow (an oscillatory shear flow driven by the oscillatory motion of a wall along its plane direction). Figure 4 shows the hybrid solution of the oscillatory velocity field corresponding to a flow with period 300τ . The spatio-temporal diagram for the velocity in Fig. 4(b) indicates that the mean values of the fluctuating MD-velocity field are perfectly coupled with the deterministic Navier–Stokes equa-

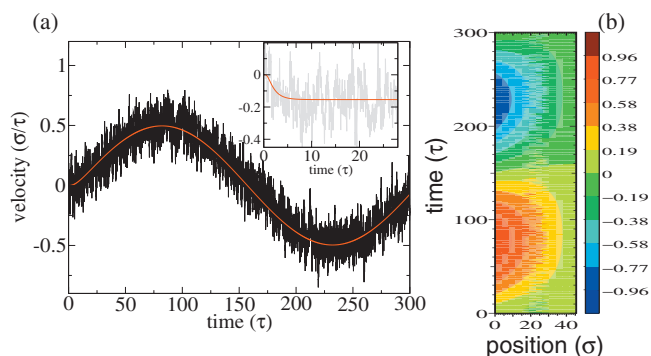


FIG. 4. (a) Time evolution of the velocity at one finite volume cell within the MD region in an oscillatory shear flow. For comparison, the deterministic Navier–Stokes solution is shown in red lines. The inset shows velocity in one MD cell at the start-up of a Couette flow. (b) Contour plot of the flow velocity in the spatio-temporal plane. The noisy region at the center of the slab corresponds to the MD region, while the outer domains were solved by deterministic continuum hydrodynamics.

tion. This is also illustrated in Fig. 4(a) by comparing the velocity at one MD cell with the corresponding deterministic solution (red solid line). The large viscosity of liquid water induces a fast transfer of momenta across the buffers. Hence, even for faster shear rates [see the inset of Fig. 4(a)], no trace of phase delay between the MD and CFD velocities was observed.⁷

C. Mass fluctuations

One of the interesting properties of the AdResS-HybridMD approach is that the MD region becomes an open system, which exchanges mass with its surroundings. As stated before, to that end, it is quite important to check that mass fluctuation across the MD border (H) is consistent with the GC prescription. We measured the mass variance inside the MD domain and compared it with the GC result, $\text{Var}[\rho] = \rho k_B T / (V c_T^2)$, where V is the system's volume and $c_T^2 = (\partial P / \partial \rho)_T$ is the squared isothermal sound velocity [related to the isothermal compressibility, $\beta_T = (c_T^2 \rho)^{-1}$]. Taking the sound velocity for the flexible TIP3P water reported in Ref. 22, $c_T = 7.38(\epsilon/m)^{1/2}$ and the mass density $\rho = 1.20m/\sigma^3$ (recall that $m = m_O$), the GC prediction for $V = 3.5 \times 6.18 \times 11.12\sigma^3$ is $\text{Var}[\rho] = 0.0187$. Inside the MD domain we obtained $\text{Var}[\rho] = 0.020 \pm 0.002$ within different slices of the same volume. This is a quite good agreement, considering the smallness of V . In a larger volume $V = 10.5 \times 6.18 \times 11.12\sigma^3$, the triple-scale result $\text{Var}[\rho] = 0.011 \pm 0.005$ is even closer to the GC prediction $\text{Var}[\rho] = 0.0108$.

D. Energy

Although in this work we do not solve the energy exchange across H, we are in position to provide some arguments indicating that this task is solvable using the *adaptive resolution buffer* setup. Energy exchange requires three properties: (1) energy should be properly defined across MD, (2) the scheme should allow to change the thermodynamic state of the system, and (3) one should be able to control the amount of energy per unit time inserted into MD. Concern-

ing (1), it is important to stress that by placing the AdResS scheme inside the buffer one ensures that the energy is a well defined quantity over the total (MD+CFD) system. Also (2) is satisfied because the *adaptive resolution buffer* setup does not rely on the specificity coarse-grained model; this means that it should be possible to change the thermodynamic state of the MD domain (e.g., the mean temperature) without recalibrating the *cg* layer (we have tested this in simulations using tetrahedral molecules). Finally, we believe that (3) is solvable, but it will require a further development of the algorithm. One possible way could be to implement the flux-boundary conditions developed in Ref. 9. We expect to present an algorithm of this sort in future works.

VI. CONCLUSIONS

To conclude, we have presented a flexible and robust hybrid scheme for hydrodynamics of molecular liquids, which combines atomistic, mesoscopic, and continuum models. This triple-scale scheme uses a flux based particle-continuum hybrid to couple the atomistic core and continuum sides of the system, while it generalizes the role of the particle buffer to allow for a gradual change in molecular resolution: from an all-atom at the core to a mesoscopic one near the buffer end. Structure and hydrodynamic of the core (MD) region were shown to be robust against changes in the choice of the mesoscopic model, greatly reducing calibration burdens. Further extensions to allow for energy exchange and multiple species will be explored in future works.

ACKNOWLEDGMENTS

We thank Anne Dejoan, Christoph Junghans, Burkhard Dünweg, and Luigi Delle Site for useful discussions. This work is supported in part by the Volkswagen foundation. R.D.-B. acknowledges additional funding from Ramón y Cajal Contract and Project No. FIS2007-65869-C03-01 funded by the Spanish Government (MEC), and also funding from the “Comunidad de Madrid” through the MOSSNOHO Project (Project No. S-0505/ESP/0299). M.P. acknowledges additional financial support through Project No. J1-2281 from the Slovenian Research Agency.

¹J. Q. Broughton, F. F. Abraham, N. Bernstein, and E. Kaxiras, *Phys. Rev. B* **60**, 2391 (1999).

²J. Rottler, S. Barsky, and M. O. Robbins, *Phys. Rev. Lett.* **89**, 148304 (2002).

³M. Praprotnik, L. Delle Site, and K. Kremer, *Annu. Rev. Phys. Chem.* **59**, 545 (2008).

⁴P. Koumoutsakos, *Annu. Rev. Fluid Mech.* **37**, 457 (2005).

⁵A. Malevanets and R. Kapral, *J. Chem. Phys.* **112**, 7260 (2000).

⁶A. Donev, B. J. Alder, and A. L. Garcia, *Phys. Rev. Lett.* **101**, 075902 (2008).

⁷R. Delgado-Buscalioni, K. Kremer, and M. Praprotnik, *J. Chem. Phys.* **128**, 114110 (2008).

⁸D. Fedosov and G. Karniadakis, *J. Comp. Physiol.* **228**, 1157 (2009).

⁹E. G. Flekkøy, R. Delgado-Buscalioni, and P. V. Coveney, *Phys. Rev. E* **72**, 026703 (2005).

¹⁰R. Delgado-Buscalioni and G. De Fabritiis, *Phys. Rev. E* **76**, 036709 (2007).

¹¹E. M. Kotsalis, J. H. Walther, E. Kaxiras, and P. Koumoutsakos, *Phys. Rev. E* **79**, 045701 (2009).

¹²J. Faraudo and F. Bresme, *Phys. Rev. Lett.* **92**, 236102 (2004).

¹³D. Frenkel and B. Smith, *Understanding Molecular Simulation: From Algorithms to Applications*, 2nd ed. (Academic, San Diego, 2002).

¹⁴G. C. Lynch and B. M. Pettitt, *J. Chem. Phys.* **107**, 8594 (1997).

¹⁵G. De Fabritiis, R. Delgado-Buscalioni, and P. Coveney, *Phys. Rev. Lett.* **97**, 134501 (2006).

¹⁶In the original HybridMD scheme molecule insertion is done using the USHER algorithm, which was originally designed for Lennard-Jones particles (Ref. 30) and water (Ref. 38).

¹⁷M. Praprotnik, L. Delle Site, and K. Kremer, *J. Chem. Phys.* **123**, 224106 (2005).

¹⁸D. Reith, M. Pütz, and F. Müller-Plathe, *J. Comput. Chem.* **24**, 1624 (2003).

¹⁹C. Junghans, M. Praprotnik, and K. Kremer, *Soft Matter* **4**, 156 (2008).

²⁰W. Tschöp, K. Kremer, J. Batoulis, T. Bürger, and O. Hahn, *Acta Polym.* **49**, 61 (1998).

²¹W. Tschöp, K. Kremer, O. Hahn, J. Batoulis, and T. Bürger, *Acta Polym.* **49**, 75 (1998).

²²G. De Fabritiis, M. Serrano, R. Delgado-Buscalioni, and P. V. Coveney, *Phys. Rev. E* **75**, 026307 (2007).

²³D. Janežič, M. Praprotnik, and F. Merzel, *J. Chem. Phys.* **122**, 174101 (2005).

²⁴M. Praprotnik, K. Kremer, and L. Delle Site, *J. Phys. A: Math. Theor.* **40**, F281 (2007).

²⁵L. Delle Site, *Phys. Rev. E* **76**, 047701 (2007).

²⁶T. Soddemann, B. Dünweg, and K. Kremer, *Phys. Rev. E* **68**, 046702 (2003).

²⁷M. Praprotnik, K. Kremer, and L. Delle Site, *Phys. Rev. E* **75**, 017701 (2007).

²⁸S. Matysiak, C. Clementi, M. Praprotnik, K. Kremer, and L. Delle Site, *J. Chem. Phys.* **128**, 024503 (2008).

²⁹M. Praprotnik, L. Delle Site, and K. Kremer, *Phys. Rev. E* **73**, 066701 (2006).

³⁰R. Delgado-Buscalioni and P. V. Coveney, *J. Chem. Phys.* **119**, 978 (2003).

³¹W. J. Briels and R. L. C. Akkerman, *Mol. Simul.* **28**, 145 (2002).

³²C. Hijón, P. Español, E. Vanden-Eijnden, and R. Delgado-Buscalioni, *Faraday Discuss.* **144**, 301 (2010).

³³W. L. Jorgensen, J. Chandrasekhar, J. D. Madura, R. W. Impey, and M. L. Klein, *J. Chem. Phys.* **79**, 926 (1983).

³⁴E. Neria, S. Fischer, and M. Karplus, *J. Chem. Phys.* **105**, 1902 (1996).

³⁵M. Praprotnik and D. Janežič, *J. Chem. Phys.* **122**, 174103 (2005).

³⁶M. Neumann, *Mol. Phys.* **50**, 841 (1983).

³⁷M. Praprotnik, S. Matysiak, L. Delle Site, K. Kremer, and C. Clementi, *J. Phys.: Condens. Matter* **19**, 292201 (2007).

³⁸G. De Fabritiis, R. Delgado-Buscalioni, and P. V. Coveney, *J. Chem. Phys.* **121**, 12139 (2004).